

# Tuning of electronic and optic anisotropy in GaAs quantum rings

Yu Liu

*SKLSM, Institute of Semiconductors, Chinese Academy of Sciences, Beijing, China*

Zhenhua Wu\*

*Key Laboratory of Microelectronics Devices and Integrated Technology,  
Institute of Microelectronics, Chinese Academy of Sciences, Beijing, China*

## Abstract

We study theoretically on electronic and anisotropy in a quantum ring formed on AlGaAs/GaAs heterostructures. We demonstrate the effective modulation of the electron distribution and optical absorption in quantum rings utilizing the interplay between the spin-orbit interactions (SOIs) and the Coulomb interaction. By tuning the SOIs and electron numbers in a quantum ring, one can change its optical property significantly.

**keywords:** A.semiconductors; D.electron-electron interactions; D.optical properties; D.spin-orbit effects

All-electrical control of spin states is an important issue in spintronics and quantum information processing.<sup>1-4</sup> Electrically tunable spin-orbit interaction<sup>5-7</sup> (SOI) provides us with an efficient way to control spin which has become one of the most influential concepts in semiconductor spintronics.<sup>8-10</sup> In the past few years, semiconductor quantum rings (QRs) have attracted intensive interests due to their unique topological geometry and energy spectrum.<sup>11-13</sup> State-of-the-art growth, etching and gate techniques have made it possible to fabricate high-quality QRs, and control the number of electrons in a QR exactly.<sup>14,15</sup> The interplay between the RSOI<sup>16-18</sup> and DSOI results in a periodic potential in an isolated QR that breaks the rotational symmetry, produces gaps in the energy spectrum and suppresses the persistent currents.<sup>19</sup> This interesting feature leads to anisotropic spin transport and could be detected using the transport property in an opened two-terminal quantum ring.<sup>20,21</sup>

In this paper, we investigate theoretically the multi-electron states in GaAs QRs in the presence of the SOIs and a perpendicular magnetic field using the configuration interaction (CI) method, which is numerically exact. The QR in the presence of the RSOI and DSOI behaves like two quantum dots coupled laterally along specific crystallographic direction, i.e.,  $[110]$  or  $[1\bar{1}0]$ . The inter-dot coupling can be tuned by changing the strengths of the SOIs. Interestingly, this anisotropic electron distribution, which can be rotate from  $[110]$  to  $[1\bar{1}0]$  direction by reversing the direction of the perpendicular electric field, results in anisotropic optical properties that provide us with a possible way to detect it experimentally.

We consider a one-dimensional (1D) GaAs QR structure schematically shown in Fig. 1 containing 3, 4, 5 and 6 electrons with considering the Coulomb interaction. In the presence of both RSOI and DSOI, we

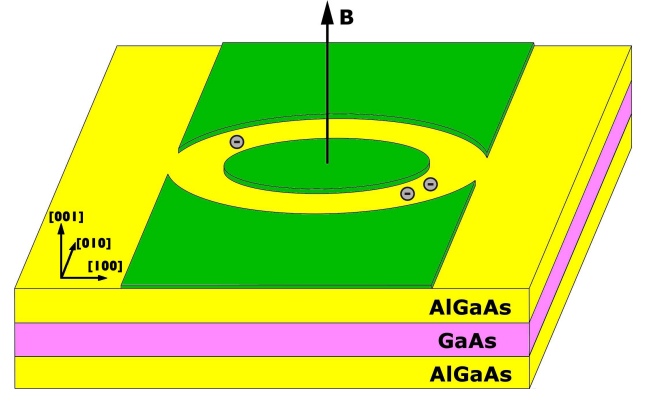


FIG. 1: (Color online) Schematic diagram of a considered multi-electron QR.

take

$$H_e = \left[ -i \frac{\partial}{\partial \varphi} + \frac{\Phi}{\Phi_0} + \frac{\bar{\alpha}}{2} \sigma_r - \frac{\bar{\beta}}{2} \sigma_\varphi(-\varphi) \right]^2 - \frac{\bar{\alpha}^2 + \bar{\beta}^2}{4} + \frac{\bar{\alpha}\bar{\beta}}{2} \sin 2\varphi + \frac{1}{2} \bar{g} b \sigma_z, \quad (1)$$

as our single electron Hamiltonian, where  $\sigma_r = \cos \varphi \sigma_x + \sin \varphi \sigma_y$ ,  $\sigma_\varphi = \cos \varphi \sigma_y - \sin \varphi \sigma_x$ ,  $\Phi = B\pi R^2$  is the magnetic flux threading the ring,  $\Phi_0 = h/e$  is the flux unit,  $b = e\hbar B/2m^*E_0$  is the dimensionless magnetic field,  $\bar{\alpha}(\bar{\beta}) = \alpha(\beta)/E_0R$  specifies the dimensionless RSOI (DSOI) strength,  $E_0 = \hbar^2/2m^*R^2$  with the ring radius  $R$ , and  $\bar{g} = g^*m^*/2m_0$  is the dimensionless  $g$  factor.<sup>19</sup> From this Hamiltonian, one can see clearly that the QR with RSOI and DSOI does not possess the rotational symmetry, because there are two potential wells at  $\phi = 3\pi/4$  and  $\phi = -\pi/4$ . Thus the QR behaves like a laterally-coupled double quantum dots.

The total Hamiltonian of the multi-electron QR can be

rewritten in second-quantization

$$H = \sum_i E_i a_i^\dagger a_i + \frac{1}{2} \gamma \sum_{ij i' j'} \langle ij | U | i' j' \rangle a_i^\dagger a_j^\dagger a_{i'} a_{j'}, \quad (2)$$

where  $E_i$  is the energy of the  $i$ -th single electron level, which can be obtained numerically by solving the single electron Schrödinger equation shown in Eq. (1). The parameter  $\gamma = e^2/4\pi\epsilon_0\epsilon$  and  $U = 1/r$ . We adopt the configuration interaction (CI) method, which is numerically exact, to calculate the eigenvalues and eigenstates of the above Hamiltonian. The total wavefunction can be expanded  $|\chi\rangle = \sum_i C_i |I\rangle$ , where the state vector  $|I\rangle = |\cdots 01_i 0 \cdots 01_j 0 \cdots\rangle = a_i^\dagger a_j^\dagger |0\rangle$ , with  $i < j$ . Here  $|0\rangle$  represents the vacuum state and  $a_i^\dagger$  ( $a_i$ ) is the electron creation (annihilation) operator of the states.  $i$  and  $j$  denoting the  $i$ -th and  $j$ -th single electron energy levels, respectively. The matrix element of the total Hamiltonian can be calculated

$$\langle I | H | J \rangle = (E_i + E_j) \delta_{ip} \delta_{jq} + \gamma [\langle ij | U | qp \rangle - \langle ij | U | pq \rangle]. \quad (3)$$

Solving the above secular equation, we can obtain the eigenenergies and the eigenstates of the multi-electron system, and calculate the electron distribution, and optical property of the multi-electron QRs.

The optical absorption rate is obtained within the electric-dipole approximation

$$\begin{aligned} W_{ab} &= \frac{2\pi}{\hbar} \sum_f |\langle f | H_{ep} | i \rangle|^2 \delta(E_f - E_i) \\ &= \frac{2\pi}{\hbar} \sum_{f,i} \left( \frac{eA_0}{m^*} \right)^2 |\langle f | \vec{\epsilon}_\lambda \cdot (\vec{p}_1 + \vec{p}_2) | i \rangle|^2 \\ &\quad \times \delta(E_f - E_i - \hbar\omega), \end{aligned} \quad (4)$$

where  $E_i$  and  $E_f$  are the energies of the initial and final states, respectively.  $H_{ep} = (e/m^*)(\vec{A} \cdot \vec{p}_1 + \vec{A} \cdot \vec{p}_2)$ , here  $\vec{p}_{1,2}$  are the canonical momenta of the electrons and  $\vec{A} = \sum_k A_0 \vec{\epsilon}_\lambda \{ a_{k\lambda} e^{i(-\omega t + \vec{k} \cdot \vec{r})} + a_{k\lambda}^\dagger e^{i(\omega t - \vec{k} \cdot \vec{r})} \}$  in which  $a_{k\lambda}$ ,  $a_{k\lambda}^\dagger$  are photon annihilation and creation operators, respectively.  $A_0$ ,  $\omega$  and  $\vec{\epsilon}_\lambda$  are the amplitude, frequency and polarization vector of the incident linear-polarized light. In the calculation we replace the energy delta function  $\delta(E_{12} - \hbar\omega)$  with a Lorentz broadened function  $(\Gamma/\pi)/((\hbar\omega - E_{12})^2 + \Gamma^2)$  where  $\Gamma$  is the broadening parameter describing the homogeneous broadening of the energy levels in the ring.

The accuracy of the calculated multi-electron energy spectrum depends on the number of possible many-particle configurations that are used which is determined by the number of electrons ( $N_e = 3, 4, 5$ , and  $6$  in this paper), and the number of single-particle states  $N_S$ . In the

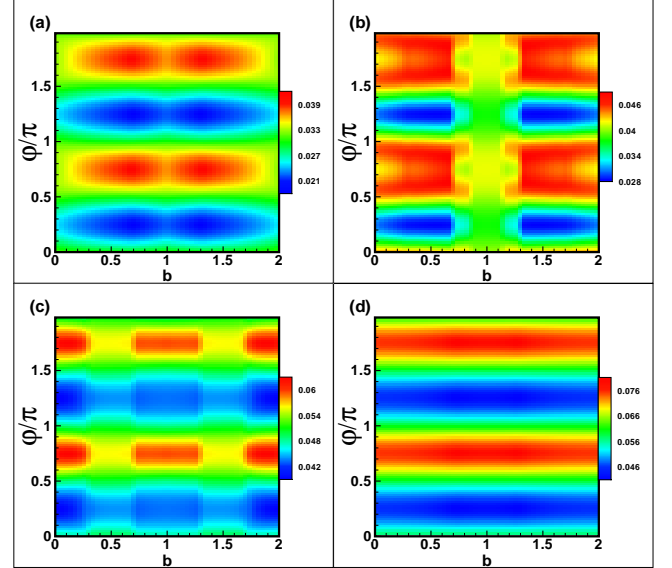


FIG. 2: (Color online) Contour plot of the electron distribution in (a) three-electron QR, (b) four-electron QR, (c) five-electron QR, (d) six-electron QR as function of magnetic field  $b$  and the crystallographic direction  $\phi$ .  $\bar{\alpha} = 2.0$ ,  $\bar{\beta} = 1.0$ .

calculation we include 30 single-particle electron states to ensure that the lower multi-electron states are numerically accurate, for instance, the accuracy of the lowest levels can approach to  $1.0 \times 10^{-4} meV$ . For simplicity, all physical quantities are taken dimensionless, e.g., the length unit is the radius of the ring  $R$ , the energy unit is  $E_0$  and the magnetic field unit is  $b$ . The relevant parameters for GaAs are:<sup>22</sup> the electron effective mass  $m^* = 0.067m_0$ , the effective  $g$ -factor  $g^* = -0.44$ , and the dielectric constant  $\epsilon = 12.5$ . For example, for  $R = 30nm$  we find  $E_0 = 0.633meV$  and  $b = 1.365$  when  $B = 1T$ .

Figure 2 depicts the contour plot of the electron distribution in multi-electron QR of different cases in the presence of both the SOIs and the Coulomb interaction. One can see that the electrons are mainly localized in a region along the specific crystallographic direction  $[1\bar{1}0]$  which makes the single QR behave like laterally-coupled double quantum dots. This is caused by the interplay between the RSOI and DSOI which breaks the rotational symmetry and results in an azimuthal periodic potential.<sup>19</sup> The behavior of electron distribution is very different with increasing magnetic field  $b$  for different electron numbers. This is caused by the differences of overlap between electrons of each single electron distribution. For three-electron case there are two kinds of possible single electron distribution: (i) two electrons are localized at  $\phi = 3\pi/4$  or  $\phi = -\pi/4$ , while the third electron localizes at the opposite side, i.e.,  $\phi = -\pi/4$  or  $\phi = 3\pi/4$ ; (ii) all three electrons localize at  $\phi = 3\pi/4$  or  $\phi = -\pi/4$ . Due to the repulsive Coulomb interaction, this configuration has higher energy, therefore the ground state of three-electron case prefers a triangular configuration. This is

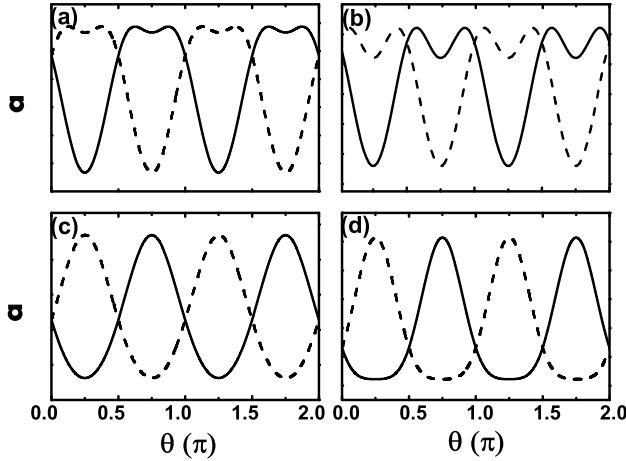


FIG. 3: The optical absorption indices  $a$  as a function of the direction of the polarized vector of the incident linear polarized light of (a) three-electron QR, (b) four-electron QR, (c) five-electron QR, (d) six-electron QR.  $\bar{\beta} = 1.0$ ,  $\bar{\alpha} = 2.0$  (the solid line),  $\bar{\alpha} = -2.0$  (the dashed line).

because the azimuthal confining potential (the third term in Hamiltonian (1)) squeezes the electron wavefunctions and forces them align along the specific crystallographic direction, i.e.,  $[1\bar{1}0]$  (see Fig. 2(a)), while the repulsive Coulomb interaction pushes two electrons away from this direction. Therefore one can see clearly that the peaks of electron distribution at  $\phi = 3\pi/4$  or  $\phi = -\pi/4$  become broadening comparing with the two-electron case (see Fig. 7 in Ref. [23]). For four and five electron QR they both have three kinds of possible single electron distribution which give more complicated features shown in Figs. 2(b) and 2(c). However, the six-electron QR shows in Fig. 2(d) releases a feature very similar with the two-electron's.<sup>23</sup> This is because the repulsive Coulomb interaction makes the ground state of six-electron case prefer a bar-bell like configuration, i.e., three electrons are localized at  $\phi = 3\pi/4$  or  $\phi = -\pi/4$ , while the other three localize at the opposite side. In this case the three electrons is too close and therefore the density distribution (see Fig. 2(d)) shows a single peak but with broadened width (see the color scales of Fig. 2).

We can switch the minima of the azimuthal periodic potential from  $[110]$  to  $[1\bar{1}0]$  rapidly by reversing the direction of the perpendicular electric field, i.e.,  $\bar{\alpha}$  to  $-\bar{\alpha}$ . The orientation of the electron distribution can be switched from  $[1\bar{1}0]$  to  $[110]$ . Besides, by tuning the external magnetic field  $b$ , we can tune the shape of the electron distribution. Thus, it provides a method to control the electron state by using SOIs and the external

magnetic field.

Next we turn to the discussion how to detect the multi-electron spatial anisotropic distribution. Previous experiments had shown that the electron spin states can be measured by the tunnelling process through quantum dots.<sup>24–26</sup> Here we propose an optical method, i.e., optical absorption in the infrared regime, to detect the electron spatial anisotropic distribution. This method is able to detect more directly the anisotropic electron distribution and the overlap factor between the ground and first excited states, i.e., anisotropic absorption. We calculate the optical absorption in the infrared regime with considering a beam of linear-polarized light incident along the  $z$  axis. In Fig. 3 we plot the optical absorption for different electron numbers as a function of the angle  $\theta$  of the polarization plane of the incident linear-polarized light with respect to the  $x$  axis at zero magnetic field. From these figures, one can find that the optical absorption oscillates periodically with increasing crystallographic angle  $\theta$  which is consistent with the electron distributions that shown in Fig. 2. Due to the azimuthal periodic potential induced by the interplay between the RSOI and DSOI and the Coulomb repulsion between these electrons the electron distributions are localized in the ring along the crystallographic direction  $\varphi = \pm\pi/4$  with different shape. These anisotropic electron distribution certainly leads to an anisotropic behavior of the optical absorption, i.e., periodical oscillation of the optical absorption as a function of the crystallographic direction  $\theta$  (see Fig. 3). By reversing the direction of the perpendicular electric field, i.e.,  $\bar{\alpha}$  to  $-\bar{\alpha}$ , the optical absorption will change strongly since the electric dipoles of these electrons change from parallel to perpendicular with respect to the polarization vector of the incident light. This large variation provides us with an efficient tool to detect the anisotropy in the electron distribution.

In summary, we demonstrate theoretically that the anisotropic distribution of multi-electron states in a semiconductor quantum ring is caused by the interplay between the Rashba SOI and Dresselhaus SOI in the presence of a perpendicular magnetic field. This property can be switched by reversing the direction of the perpendicular electric field and detected by utilizing the optical absorption. Our theory provides a new way to control electron state and optical property of nanostructures by electrical means.

### Acknowledgments

This work was supported by the Opening Project of KLMEIT, IMECAS.

\* Electronic address: wuzhenhua@ime.ac.cn

<sup>1</sup> S. A. Wolf, D. D. Awschalom, R. A. Buhrman, J. M.

- Daughton, S. von Molnár, M. L. Roukes, A. Y. Chtchelkanova, and D. M. Treger, *Science* **294**, 1488 (2001).
- <sup>2</sup> Tapash Chakraborty and Pekka Pietiläinen, *Phys. Rev. B* **71**, 113305 (2005).
  - <sup>3</sup> Pekka Pietiläinen and Tapash Chakraborty, *Phys. Rev. B* **73**, 155315 (2006).
  - <sup>4</sup> M. Ciorga, A. Wensauer, M. Pioro-Ladriere, M. Korkusinski, J. Kyriakidis, A. S. Sachrajda, and P. Hawrylak, *Phys. Rev. Lett.* **88**, 256804 (2002).
  - <sup>5</sup> D. Grundler, *Phys. Rev. Lett.* **84**, 6074 (2000).
  - <sup>6</sup> J. Nitta, T. Akazaki, H. Takayanagi, and T. Enoki, *Phys. Rev. Lett.* **78**, 1335 (1997).
  - <sup>7</sup> M. König, A. Tschetschetkin, E. M. Hankiewicz, J. Sinova, V. Hock, V. Daumer, M. Schäfer, C. R. Becker, H. Buhmann, and L. W. Molenkamp, *Phys. Rev. Lett.* **96**, 076804 (2006).
  - <sup>8</sup> I. Žutić, J. Fabian, and S. D. Sarma, *Rev. Mod. Phys.* **76**, 323 (2004).
  - <sup>9</sup> R. Winkler, *Physica E* **22**, 450 (2004).
  - <sup>10</sup> S. Datta and B. Das, *Appl. Phys. Lett.* **56**, 665, (1990).
  - <sup>11</sup> Junsaku Nitta, Frank E. Meijer, and Hideaki Takayanagi, *Appl. Phys. Lett.* **75**, 695 (1999).
  - <sup>12</sup> P. Földi, M. G. Benedict, O. Kálmán, and F. M. Peeters, *Phys. Rev. B* **80**, 165303 (2009).
  - <sup>13</sup> L. K. Castelano, G. -Q. Hai, B. Partoens, and F. M. Peeters, *Phys. Rev. B* **78**, 195315 (2008).
  - <sup>14</sup> R. C. Ashoori, *Nature (London)* **379**, 413 (1996).
  - <sup>15</sup> S. Tarucha, D. G. Austing, T. Honda, R. J. van der Hage, and L. P. Kouwenhoven, *Phys. Rev. Lett.* **77**, 3613 (1996).
  - <sup>16</sup> W. Yang, and Kai Chang, *Phys. Rev. B* **74**, 193314 (2006).
  - <sup>17</sup> W. Yang, and Kai Chang, *Phys. Rev. B* **73**, 113303 (2006).
  - <sup>18</sup> W. Yang, Kai Chang and S. C. Zhang, *Phys. Rev. Lett.* **100**, 056602 (2008).
  - <sup>19</sup> J. S. Sheng and Kai Chang, *Phys. Rev. B* **74**, 235315 (2006).
  - <sup>20</sup> Miao Wang and Kai Chang, *Phys. Rev. B* **77**, 125330 (2008).
  - <sup>21</sup> Miao Wang and Kai Chang, *Appl. Phys. Lett.* **94**, 052108 (2009).
  - <sup>22</sup> *Physics of Group IV Elements and III-V Compounds*, Landolt-Börnstein (New Series) Group III Vol. 17, edited by O. Madelung (Springer-Verlag, Berlin, 1982).
  - <sup>23</sup> Y. Liu, F. Cheng, X. J. Li, F. M. Peeters, and Kai Chang, *Phys. Rev. B* **82**, 045312 (2010).
  - <sup>24</sup> R. Hanson, L. M. K. Vandersypen, L. H. Willems van Beveren, J. M. Elzerman, I. T. Vink, and L. P. Kouwenhoven, *Phys. Rev. B* **70**, 241304(R) (2004).
  - <sup>25</sup> K. Hitachi, M. Yamamoto, and S. Tarucha, *Phys. Rev. B* **74**, 161301(R) (2006).
  - <sup>26</sup> T. Hatano, M. Stopa, and S. Tarucha, *Science*, **309**, 268 (2005).